

# Dark energy records in lensed cosmic microwave background

Viviana Acquaviva<sup>1,2</sup>, Carlo Baccigalupi<sup>1,2,3</sup>

<sup>1</sup> *SISSA/ISAS, Astrophysics Sector, Via Beirut, 4, I-34014 Trieste, Italy*

<sup>2</sup> *INFN, Sezione di Trieste, Via Valerio 2, I-34014 Trieste, Italy*

<sup>3</sup> *Institut für Theoretische Astrophysik, Universität Heidelberg, Albert-Überle-Strasse 2, D-69120 Heidelberg, Germany*

We consider the weak lensing effect induced by linear cosmological perturbations on the cosmic microwave background (CMB) polarization anisotropies. We find that the amplitude of the lensing peak in the BB mode power spectrum is a faithful tracer of the dark energy dynamics at the onset of cosmic acceleration. This is due to two reasons. First, the lensing power is non-zero only at intermediate redshifts between the observer and the source, keeping record of the linear perturbation growth rate at the corresponding epoch. Second, the BB lensing signal is expected to dominate over the other sources. The effect on the total intensity, EE polarization spectra and their correlation is sensibly smaller since they are dominated by primary anisotropies.

We investigate and quantify the effect by means of exact tracking quintessence models, as well as parameterizing the dark energy equation of state in terms of the present value ( $w_0$ ) and first derivative in scale factor ( $w_a$ ); in the interval allowed by the present constraints on dark energy, the variation of  $w_a$  induces a change in the BB mode lensing amplitude as large as 30%. A Fisher matrix analysis, under conservative assumptions concerning the increase of the sample variance due to the non-Gaussian statistics of lensing in the BB power, shows that a 10% precision on both  $w_0$  and  $w_a$  is achievable from the CMB power spectra by the forthcoming experiments capable to detect the lensing peak in CMB polarization. These results show that the CMB can probe the differential redshift behavior of the dark energy equation of state, beyond its average.

## I. INTRODUCTION

One of the most challenging issues in modern cosmology is the comprehension of the nature of the dark energy, the unknown component representing about 70% of the cosmological critical density today, responsible for a late phase of acceleration in the cosmic expansion (see [1, 2] and references therein).

The first report on the evidence of cosmic acceleration was due to the magnitude-redshift relation inferred by type Ia supernovae [3, 4]; the cosmic microwave background (CMB) experiments, combined with the data on large scale structure, confirmed and strengthened that result (see [5] and references therein).

The simplest interpretation for the acceleration can be given in terms of a Cosmological Constant, leading however to serious theoretical problems concerning its magnitude. In fact, its energy scale is required to be 123 orders of magnitude lower than the Planck energy, possibly the only one relevant in the very early universe; and its value has to be such to render it comparable with the matter density at the present epoch. These issues are known as fine-tuning and coincidence, respectively.

The concept of dark energy generalizes the Cosmological Constant, allowing dynamics of the equation of state and fluctuations of the dark en-

ergy component, in the attempt to alleviate these tweaking problems and to find clues to unveil the physical mechanism giving rise to the acceleration. This is the case of the Quintessence, a self-interacting scalar field evolving according to different potential energies. For reference, the potentials which have been studied extensively in the literature are characterized by an exponential shape [6], inverse power law [7], or a combination of those [8], and have been suggested in the context of particle physics beyond the standard model.

The present measurements are consistent with the Cosmological Constant case,  $w = -1$  [9], with a precision of about ten percent. However, these observations do not have the capability to address the dynamics of the dark energy yet: the corresponding constraints either concern models where the dark energy is constant, or may be interpreted as constraints on the redshift average of the equation of state.

Most dark energy models, including the ones cited above, may account for a present equation of state close to the Cosmological Constant case, but have a significantly different evolution at the epoch of equality between dark matter and energy, occurring at redshift  $z \simeq 0.5$ . Therefore, on the basis of the Cosmological Constant problems, and having no other theoretical clue about the nature of the dark energy, it is clearly crucial to investigate its behavior at the onset of acceleration, where

the models most differ; this is the context of the present work.

The lensing effect is a unique tool for this purpose. The reason is an elementary geometric property of lensing, yielding a null cross section if the lens position coincides with the observer or the source, thus probing intermediate regions only (see [10] for reviews). The weak lensing in cosmology, i.e. the large scale shear injected on the background light by forming cosmological structures, is one of the most promising observables for future studies on dark matter and energy; a great effort is directed toward the study of the ellipticity induced by weak lensing on distant galaxies in the optical band, and how that is sensitive to the dark energy properties and other cosmological parameters. See [11] for reviews on the existing observations and future projects, [12, 13, 14, 15] for parameter forecasts, also in connection with the constraints expected from other cosmological probes.

In particular, if the source is at infinity, the lensing cross section is non-zero at redshifts roughly between 0.1 and 10, peaking at  $z \simeq 1$ . This is the case of this work, where we consider the lensing of the CMB [16, 17]. We focus on the CMB polarized signal, and in particular on the curl or BB component. Because of lensing, the gradient component of CMB polarization leaks into the BB modes, causing a broad peak centered on the angular scales of a few arcminutes, roughly corresponding to a multipole  $l \simeq 1000$ . Although the lowest expected contribution to the CMB anisotropies, this observable is entirely caused by lensing, and basically unbiased by primordial power; a contamination due to primordial gravitational waves may arise on larger angular scales, multipoles of about 100, where however the lensing signal is rapidly decreasing approaching the super-horizon regime. Moreover, the lensing is a non-Gaussian process, correlating cosmological perturbations on different angular scales, while the primordial tensor power is expected to be close to Gaussian. This difference might be crucial to deconvolve the two patterns [18]. The non-Gaussian distribution of lensing has an impact already at the level of the variance in the angular power spectrum, which is currently under investigation [19, 20, 21].

Therefore, we expect a considerable improvement in the CMB capability of constraining the dark energy dynamics at the epoch of equivalence with matter with the introduction of the BB modes analysis; our aim here is to investigate and quantify this issue. An analogous occurrence has been demonstrated considering the CMB third order

statistics in total intensity anisotropies, which is also induced by lensing only, if the primordial perturbations are perfectly Gaussian [22].

Our treatment is based on a previous work [23], casting the cosmological weak lensing theory in the context of scalar field dark energy models with arbitrary kinetic and potential energy densities, and also coupling arbitrarily to the Ricci scalar. The aim of that work was to embrace the most general scalar field dark energy models, including as a particular case the minimally coupled, purely self-interacting Quintessence, which is the subject of the present work. In section II we recall the relevant issues concerning the lensing computation in dark energy cosmologies. In section III we derive and discuss the lensed CMB power spectra and their dependence on the dynamical dark energy properties. In section IV we evaluate the impact on a parametric analysis of CMB data. Finally, in section V we draw our conclusions.

## II. WEAK LENSING AND DARK ENERGY

In this section we describe the cosmological models we consider throughout this paper, and we outline the physics of lensing on the CMB total intensity and polarization anisotropies; for more details, see [23] and references therein. We focus on the modifications to the Boltzmann codes which numerically evolve cosmological perturbations required in order to take into account the effects of lensing in scalar field dark energy cosmologies.

### A. Dark energy cosmology

The set of relevant cosmological parameters is naturally widened when one considers dark energy or modified gravity as an alternative to the Cosmological Constant. The first step is the selection of the models that we take into account. Our framework is set by the very generic action

$$S = \int d^4x \sqrt{-g} [f(\phi, R)/2\kappa - \omega(\phi)\phi^{;\mu}\phi_{;\mu}/2 - V(\phi) + \mathcal{L}_{\text{fluid}}] , \quad (1)$$

originally introduced in [24];  $\kappa = 8\pi G_*$  is the bare gravitational constant (see [25] and references therein),  $\phi$  is a classical scalar field and  $\mathcal{L}_{\text{fluid}}$  encodes the contributions from all the other components. This includes four main categories of models: *generalized gravity*, featuring

a non-canonical dependence on the Ricci scalar and no scalar field in the Lagrangian, *ordinary Quintessence*, where the gravitational sector of the action is the one of General Relativity and we allow for the presence of a dynamical scalar field with a suitable potential, *scalar-tensor theories*, where we change the gravitational coupling of the Ricci scalar but let a Cosmological Constant account for the dark energy, and some combination of these two mechanisms, often referred to as *Extended Quintessence* models [26]. Some weak lensing observables in scalar-tensor theories have been treated in [27].

It has been already pointed out [23] that in these models we have two types of deviations from the Cosmological Constant behavior. The first is seen as a difference in the expansion history, whose most immediate effect is a change in the measures of distance; the second is a change in the gravitational potential due to the interactions with the fluctuations in the scalar field, and, in scalar-tensor theories and in Extended Quintessence models, the presence of a new degree of freedom (namely the difference between the gravitational potentials  $\Phi$  and  $\Psi$ ) known as *anisotropic stress*.

In this paper we consider the tracking Quintessence scenarios. The associated action is of the form:

$$S = \int d^4x \sqrt{-g} \cdot \left[ \frac{1}{2\kappa} R - \phi^{;\mu} \phi_{;\mu} \frac{1}{2} - V(\phi) + \mathcal{L}_{\text{fluid}} \right]. \quad (2)$$

We chose two representative models where the equation of state has a mild and violent redshift behavior, respectively for the inverse power law potentials, (IPL [7]) and those inspired by supergravity theories (SUGRA [8]):

$$V(\phi) = \frac{M^{4+\alpha}}{\phi^\alpha}, \quad V(\phi) = \left( \frac{M^{4+\alpha}}{\phi^\alpha} \right) e^{4\pi G \phi^2}. \quad (3)$$

These scalar field dark energy models are implemented and integrated exactly, also considering Quintessence fluctuations, in a modification of the Boltzmann code for numerical integration of cosmological background and linear perturbations based on the version 4.0 of CMBfast [28], which has been used in several papers, see [29, 30] and references therein.

For what concerns the background evolution, a variety of models including the ones above are well described by essentially two parameters: those are the present value  $w_0$  of the equation of state and

its first derivative with respect to the scale factor  $a$ ,  $-w_a$  [31]. In this framework, the evolution of the equation of state with the scale factor is given by

$$w(a) = w_0 + w_a(1 - a) = w_\infty + (w_0 - w_\infty)a, \quad (4)$$

where  $w_\infty$  is the asymptotic value of  $w$  in the past. We will exploit the parameterization above in Section IV, in order to evaluate the precision achievable on the measure of  $w$  and  $w_\infty$  from the CMB total intensity and polarization angular power spectra.

## B. Weak lensing and Boltzmann numerical codes in cosmology

The effect of gravitational lensing on the CMB spectra had been first introduced in the CMBfast code by Zaldarriaga and Seljak [17] for Cold Dark Matter cosmologies including a Cosmological Constant ( $\Lambda$ CDM). In their formalism the effect on the correlation functions can be understood as the convolution of the unlensed spectra with a Gaussian filter determined by the *lensing potential* [10], and they show that one can safely keep only the first two terms of the corresponding Taylor expansion. The expression for the lensing potential has to be generalized in scalar-tensor cosmologies because of the presence of anisotropic stress already at a linear level [23]. In the present scenario, however, this is not required and the structure of the quantities relevant for computing the lensing effect is formally unchanged. The first two terms in the Taylor expansion of the lensing correlation function [17] are given by

$$\sigma_0^2(\theta) = 16\pi^2 \int_0^{\chi_{\text{rec}}} W^2(\chi, \chi_{\text{rec}}) d\chi \int_0^\infty k^3 dk \cdot P_\phi(k, \tau = \tau_0 - \chi) [1 - J_0(k\theta\chi)], \quad (5)$$

and

$$\sigma_2^2(\theta) = 16\pi^2 \int_0^{\chi_{\text{rec}}} W^2(\chi, \chi_{\text{rec}}) d\chi \int_0^\infty k^3 dk \cdot P_\phi(k, \tau = \tau_0 - \chi) J_2(k\theta\chi), \quad (6)$$

where  $k$  is the wavenumber,  $J_l$  is the Bessel function of order  $l$ ,  $\chi$  is the comoving radial distance,  $\tau$  is the conformal time,  $P_\phi$  is the power spectrum of the gravitational potential, and  $W$  is a function accounting for the cosmic curvature, which amounts to  $1 - \chi/\chi_{\text{rec}}$  for a flat universe. In  $\Lambda$ CDM cosmologies and most of the numerical codes dealing with them, including CMBfast, the quantities

appearing in the above equations may be computed independently of the main routine which performs the integration of the hierarchical Boltzmann equations. This can be done because the power spectrum of matter density perturbations  $\Delta_m$  can be factorized in two terms, depending respectively only on the wavenumber and the redshift:

$$P_{\Delta_m}(k, \chi) = Ak^n \cdot T^2(k, 0)g^2(\chi) . \quad (7)$$

$Ak^n$  here represents the primordial power,  $T$  is the transfer function of density perturbations taking into account the evolution on sub-horizon scales, and  $g$  is the overall linear growth factor. However, this separation relies crucially on the assumption that only one component is fluctuating, namely the CDM, and leads to a substantial numerical simplification because a satisfactory analytical fit for the linear growth of the perturbations exists [32].

This cannot be done anymore in the present scenarios, unless we ignore the influence of Quintessence perturbations, which do make a non-negligible effect on large scales [33]. To account for these changes, we evaluate numerically the gauge invariant expression of density perturbations from all fluctuating components  $\Delta$  [34]. This quantity is computed and saved while the main routine performs the integration of the hierarchical Boltzmann equations, and used later for the numerical integration of the quantities (5) and (6), which include all fluctuating components.

A separate issue concerns the normalization constant  $A$  above when lensing is taken into account. The lensed perturbation spectra no longer depend linearly on the primordial normalization, since the lensing is a second order effect; consequently, the normalization has to be treated as the other parameters, having no trivial impact on the perturbations. In Section III the models under examination have been set to have the same amplitude of the primordial perturbations, in order to highlight the differences arising due to the later lensing dynamics, while in Section IV the primordial normalization is among the cosmological parameters to be constrained.

### III. LENSED CMB POLARIZATION POWER SPECTRA

In this section we describe the phenomenology of the two dark energy models discussed in the previous Section, as they well represent the different

dynamics that the dark energy might have. We study the behavior of the relevant lensing quantities, showing results for the corresponding lensed CMB power spectra. In particular, we focus on the effect induced by the dark energy behavior at the epoch when the lensing power injection is effective. We give a qualitative description of how the lensing peak breaks the degeneracy between  $w_0$  and  $w_\infty$  affecting the TT, TE and EE spectra. Both the SUGRA and the IPL models are characterized by two parameters, the index of the power-law  $\alpha$ , and the mass of the field  $M$ . As it is well known [35, 36] they both admit attractor trajectories for the field dynamics in the early universe, known as tracking solutions. These are characterized by a relative independence of the field dynamics on its mass. The relevant parameter ruling the motion of the field is  $\alpha$ . On the other hand, the mass sets the normalization of the dark energy density along the trajectory, being therefore crucial to achieve acceleration today, and must be set accordingly.

First of all we want to discuss qualitatively the effects on the corresponding background evolution, where we expect to see the most relevant differences between the two models; the key point of the comparison is the behavior of the dark energy component, which will characterize the scaling of the expansion factor. We consider models where the present equation of state of the dark energy is  $w_0 = -0.9$ , in agreement with the present constraints [9]. The redshift evolution of  $w(z)$  is shown in Fig. 1, showing that while in the IPL model it is mildly departing from its present value at high redshifts, in the SUGRA one there is rapidly gets to higher values. The remaining cosmological parameters, are chosen accordingly to the concordance model, see the first column of table I.

Since in the SUGRA model the dark energy becomes relevant at higher redshifts with respect to the  $\Lambda$ CDM and IPL cases, the inhibition of structure formation starts earlier (see [37] and references therein); thus, for a fixed primordial normalization, we expect two effects. The first is a smaller lensing signal, as a result of the relevant window of redshifts being peaked at  $z \simeq 1$  for CMB lensing (see [10]). The second is the lensing peaking at earlier epochs, in consequence of the structure formation process occurring at higher redshift following the earlier dark energy dominance.

These features can be verified analyzing the function  $\sigma_0(\theta)$ ; we choose a reference value of the angle, say  $\theta = 4 \cdot 10^{-3}$  radians, corresponding roughly to the middle of the range suitable for CMB compu-

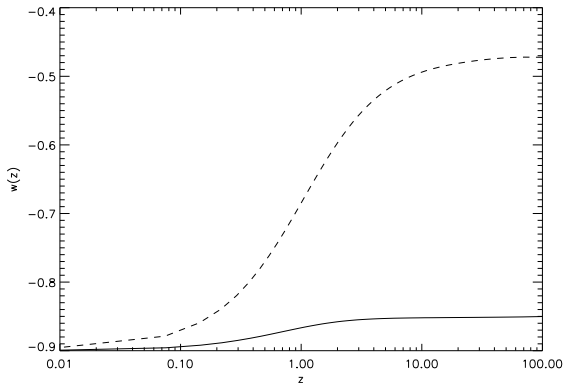


FIG. 1: Evolution of the equation of state of dark energy for the SUGRA (dashed line) and IPL (solid line) models.

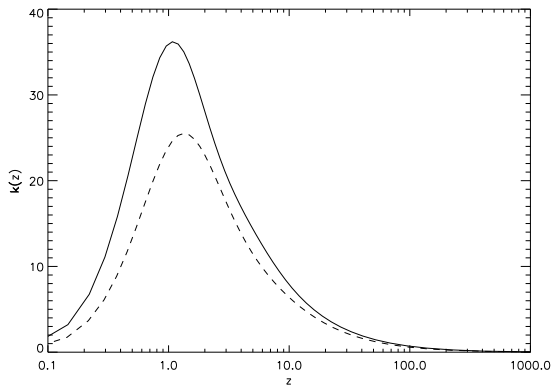


FIG. 2: Lensing kernel for  $\theta = 4 \cdot 10^{-3}$  rad, for the SUGRA (dashed line) and IPL (solid line) models, having the same equation of state today.

tations. We plot  $\sigma_0(\theta)$  assuming a unitary power spectrum for the gravitational potential fluctuations. We call this quantity the *lensing kernel*,  $k(\theta)$ ; its dimensions are the inverse of a volume, and it gives a measure of the whole lensing effect coming from the background. The result is shown in Fig. 2. An analogous behavior is expected for  $\sigma_2(\theta)$ . Both our expectations are verified; note how the two cosmological models, although having the same values of all cosmological parameters today, differ substantially (30%) at the epoch of structure formation entirely because of the behavior of the equation of state. Note also how the lensing selects precisely that epoch.

Let us now turn to analyze the impact of the different perturbation growth rate, influencing  $\sigma_0(\theta)$  and  $\sigma_2(\theta)$  through the power spectrum of the grav-

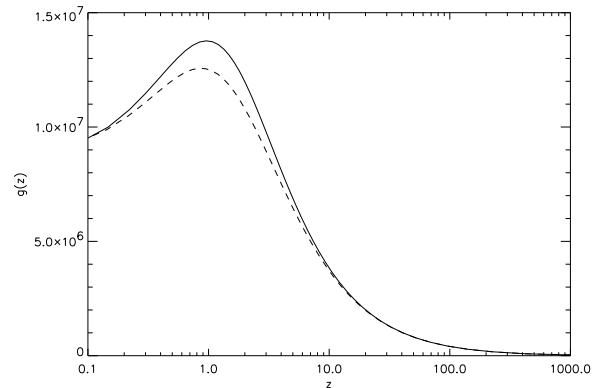


FIG. 3: Growth factor of the perturbations for a comoving wavenumber  $k = 0.1 \text{ Mpc}^{-1}$ , for the SUGRA (dashed line) and IPL (solid line) models. In the two models,  $g$  has the same value at infinity.

itational potential. It is convenient to plot the linear growth factor,  $g(\tau)$ , for the two models at a fixed wavenumber; the behavior is qualitatively the same for any  $\kappa$ . The result is shown in Fig. 3. The phenomenology is the following. In the matter dominated era, say at redshifts between 1000 and a few in the figure,  $g$  has the well known scaling as  $a = 1/(1+z)$ . At the onset of acceleration, its growth is inhibited and eventually it starts to decrease. As expected, this effect is stronger in the SUGRA case, as dark energy dominance takes place earlier. At present, the two curves tend to join again approaching the same regime in the expansion rate. The effect is of the order of 10%, featuring a trend similar to the one in Fig. 2. We thus expect a significant dependence of the amplitude of CMB lensing power upon the dark energy equation of state value at structure formation.

On the basis of the issues outlined above, it is crucial to fix CMB observables purely sourced by gravitational lensing. The BB modes in the CMB represent an almost ideal candidate for this, as the lensing is the only known mechanism adding power on all scales beyond a few hundreds where the imprint of primordial gravitational waves might be. In the following we give a qualitative illustration of its relevance, leaving a more quantitative discussion for the next Section.

The TT, TE and EE CMB spectra are dominated by primary anisotropies, imprinted at last scattering, where in most models the dark energy is not yet effective. The lensing only contributes smearing out a bit the acoustic peaks, and moving some power to the damping tail [17]. The location of the acoustic peaks depends on the different cosmolog-

ical expansion histories, as a result of the modification in the comoving distance to last scattering  $d_{LS}$ , which is written as

$$d_{LS} = H_0^{-1} \int_0^{z_{LS}} dz [\Omega_m (1+z)^3 + (1-\Omega_m) e^3 \int_0^z dz' \frac{1+w(z')}{1+z'}]^{-1/2}. \quad (8)$$

where  $H_0$  is the Hubble parameter,  $\Omega_m$  is the matter abundance today relative to the critical density and the contributions from radiation and curvature are neglected. It does not come as a surprise that this quantity depends very weakly on different forms of  $w(z)$ , since those are washed out by two integrals in redshift. The Integrated Sachs-Wolfe effect (ISW) acts on large scales only, responding to the change in the cosmic equation of state; although promising results may be obtained correlating the ISW with the large scale structure data [38], from a pure CMB point of view the cosmic variance represents a substantial limiting factor.

The BB phenomenology is utterly different. Here the lensing is the only source of power on sub-degree angular scales, and the lensing cross section is largest at structure formation, where the dark energy might differ significantly from a Cosmological Constant, even for the same expansion rate today. The lensed CMB power spectra are shown in Figs. 4, 5, 6. It is immediately evident how the sensitivity of the BB power to the dark energy at high redshifts is dramatically altered with respect to the tiny projection affecting all the other spectra. Indeed, the BB peak traces directly the perturbation growth rate and background expansion at the epoch of structure formation. For the cosmological parameters at hand, the effect is of the order of several ten percent, consistently with the results in Figs. 2, 3. We remark that the  $C_l$ s have been obtained with the same value of all cosmological parameters, including the primordial normalization, and differ only in the value of the dark energy equation of state at intermediate redshifts. We also stress that the variation of any of the usual cosmological parameters would affect equivalently the BB modes and the other spectra, as those represent parameters which are global in space and time. The dark energy equation of state is the only background quantity which may be time varying. Therefore, the effect outlined in Figs. 2, 3 is an unique signature of the different dark energy behavior, not reproducible with combinations of the other cosmological parameters. To make the projection degeneracy breaking more apparent, let's consider dark energy models featuring the same

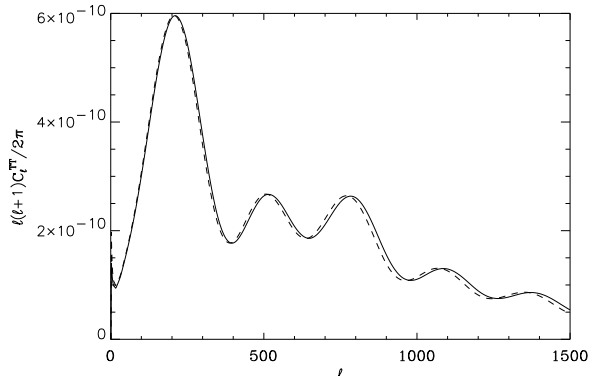


FIG. 4: TT lensed power spectra for the SUGRA (dashed line) and IPL (solid line) models.

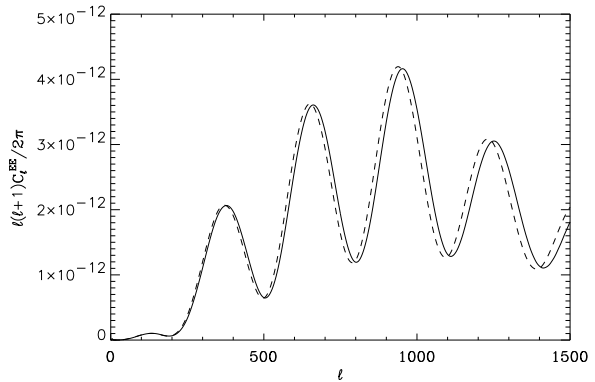


FIG. 5: EE lensed power spectra for the SUGRA (dashed line) and IPL (solid line) models.

value of  $d_{ls}$  in (8), with different values of  $w_0$  and  $w_\infty$ . The TT and BB spectra are shown in Figs. 7, 8, showing clearly the same pattern in the TT acoustic peaks but markedly different BB amplitude, reflecting the enhanced dependence of the latter on  $w_\infty$ . We will quantify the relevance of this effect in the next Section.

#### IV. FISHER MATRIX ANALYSIS

Here we give a first quantitative evaluation of the benefit that the knowledge that the BB spectra has on the CMB capability of constraining the dark energy dynamics. Our approach is based on a Fisher matrix analysis, reviewed in Section IV A; in Section IV B we show the results.

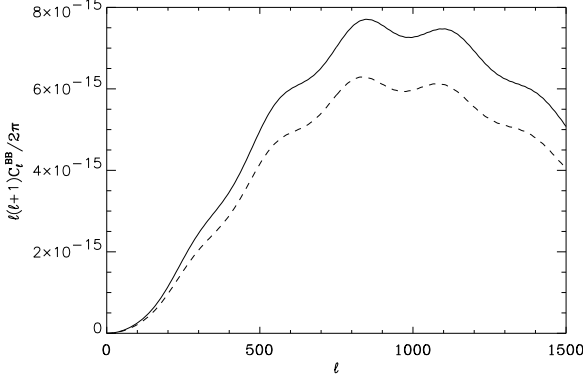


FIG. 6: BB lensed power spectra for the SUGRA (dashed line) and IPL (solid line) models.

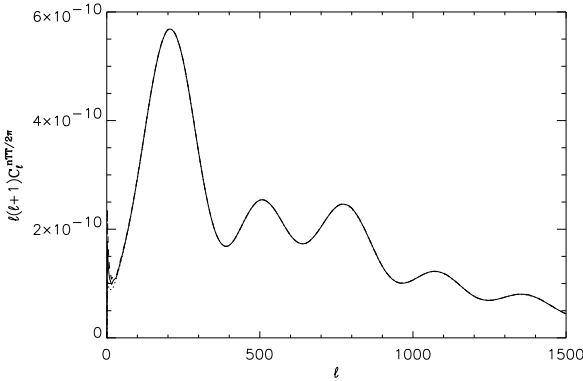


FIG. 7: Lensed TT power spectra for dark energy models with  $w_0 = -0.9$ ,  $w_\infty = -0.4$  (solid line),  $w_0 = -0.965$ ,  $w_\infty = -0.3$  (dashed line),  $w_0 = -0.8$ ,  $w_\infty = -0.56$  (dotted line).

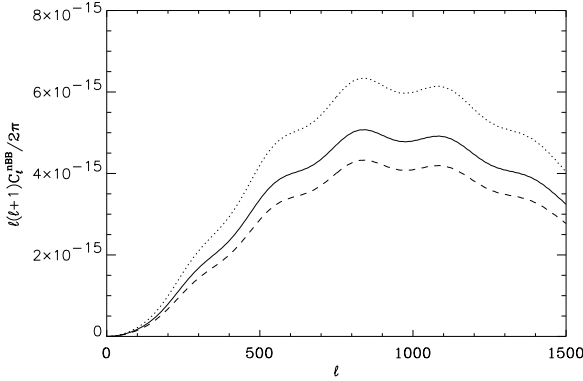


FIG. 8: Lensed BB power spectra for dark energy models with  $w_0 = -0.9$ ,  $w_\infty = -0.4$  (solid line),  $w_0 = -0.965$ ,  $w_\infty = -0.3$  (dashed line),  $w_0 = -0.8$ ,  $w_\infty = -0.56$  (dotted line).

## A. Method

In a CMB analysis involving the polarization power spectra [39], the Fisher matrix takes the form

$$F_{ij} = \sum_{\ell} \sum_{XY} \frac{\partial C_{\ell}^X}{\partial \alpha_i} [\Xi_{\ell}]_{XY}^{-1} \frac{\partial C_{\ell}^Y}{\partial \alpha_j}, \quad (9)$$

where  $X$  and  $Y$  are either TT, EE, TE or BB and  $\Xi_{XY} \equiv \text{Cov}(C_{\ell}^X C_{\ell}^Y)$  is the power spectra covariance matrix:

$$\Xi_{\ell} = \begin{pmatrix} \Xi_{\ell}^{TT,TT} & \Xi_{\ell}^{TT,EE} & \Xi_{\ell}^{TT,TE} & 0 \\ \Xi_{\ell}^{TT,EE} & \Xi_{\ell}^{EE,EE} & \Xi_{\ell}^{EE,TE} & 0 \\ \Xi_{\ell}^{TT,TE} & \Xi_{\ell}^{EE,TE} & \Xi_{\ell}^{TE,TE} & 0 \\ 0 & 0 & 0 & \Xi_{\ell}^{BB,BB} \end{pmatrix}. \quad (10)$$

The terms in the power spectra covariance matrix are given by

$$\begin{aligned} \Xi_{\ell}^{xy,x'y'} &= \frac{1}{(2\ell+1)f_{sky}\Delta\ell} \\ &\times [(C_{\ell}^{xy} + N_{\ell}^{xy})(C_{\ell}^{y'x'} + N_{\ell}^{y'x'}) \\ &\quad + (C_{\ell}^{xx'} + N_{\ell}^{xx'})(C_{\ell}^{yy'} + N_{\ell}^{yy'})] \end{aligned} \quad (11)$$

where  $(x, y) = (T, E, B)$ . The noise covariance is given by  $N_{\ell}^{xy}$ , which also contains the effect of the instrumental beam, assumed Gaussian and circular. The inverse of the Fisher matrix gives the uncertainty on the theoretical parameters:

$$C_{ij} \equiv \langle \Delta\alpha_i \Delta\alpha_j \rangle = F_{ij}^{-1}. \quad (12)$$

$\Delta\alpha_i$  is the marginalized 1- $\sigma$  error on the  $i^{\text{th}}$  parameter, and is given by the square root of the diagonal elements of the inverse of the Fisher matrix.

As a representative of the forthcoming CMB polarization probes capable to detect the BB spectrum we consider the E and B Experiment (EBEx [40]). We consider a Gaussian beam with 8 arcminutes full width half maximum, considering multipoles up to  $l = 1500$ . We also take an instrumental error corresponding to 5% of the lensing amplitude at the peak; we also assume a sky coverage of 350  $\text{deg}^2$  and we use adequately spaced band powers in  $l$ . The resulting error on the BB modes, including the cosmic variance and instrumental noise, is given in Fig. 9 for the reference  $\Lambda\text{CDM}$  model specified in table I.

A delicate issue in applying a Fisher matrix analysis to the CMB lensing is represented by the non-Gaussianity of the lensing effect, due to the correlation of cosmological perturbations on different angular scales; the lensing statistics have been

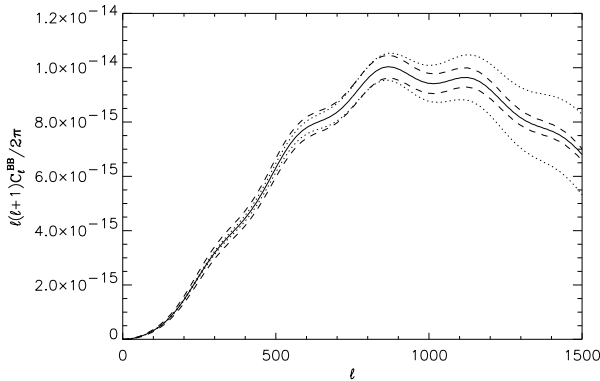


FIG. 9: The uncertainty in the  $\mathcal{C}^{BB}$  power spectrum (solid line) for the  $\Lambda$ CDM model specified in table (I), including instrumental noise (dotted line) and cosmic variance (dashed line).

recently receiving increasing attention in view of the incoming precision polarization experiments [18, 19, 20, 21].

In particular, Smith et al. [20] achieved a first quantification of the increase in the covariance matrix due to the non-Gaussian nature of the lensing signal in the BB modes, giving a pipeline to estimate the resulting achievable accuracy.

For our study their most relevant result is the behavior of the so called *degradation factor*, the ratio between the squared sample covariance in the case of this non Gaussian signal and the corresponding Gaussian case. This is shown to depend both on the instrumental error (the degradation increases with the signal-to-noise ratio of the experiment, as expected because the instrumental error is close to Gaussian) and on the maximum available multipole (again increasing with  $l_{max}$ , because of the stronger effect of the correlation between neighboring band powers).

According to their worst case scenario, we make a conservative choice enlarging by a factor 10 the covariance contribution to the BB spectrum in the covariance matrix (11); this would correspond to an experiment with  $l_{max} = 2000$  and  $\theta_{FWHM} \simeq 1'$ .

### B. Marginalized errors on cosmological parameters

We analyze two cosmological models, correspond to a pure  $\Lambda$ CDM and a SUGRA one, specified by eight cosmological parameters, including the two specifying the dark energy equation of state:

TABLE I: Results from the Fisher matrix analysis for the two models under examination.

	$\Lambda$ CDM		SUGRA	
	value	$\sigma_{Fisher}$	value	$\sigma_{Fisher}$
$w_0$	-1.	0.13	-0.9	$4.7 \times 10^{-2}$
$w_a$	-1.	0.14	-0.4	$2.2 \times 10^{-2}$
$\Omega_b h^2$	0.022	$7.5 \times 10^{-5}$	0.023	$7.0 \times 10^{-5}$
$\Omega_m h^2$	0.11	$7.1 \times 10^{-4}$	0.12	$4.3 \times 10^{-4}$
$h$	0.72	$5.9 \times 10^{-2}$	0.72	$1.3 \times 10^{-2}$
$n_S$	0.96	$2.5 \times 10^{-3}$	0.96	$2.1 \times 10^{-3}$
$\tau$	0.11	$3.1 \times 10^{-3}$	0.11	$3.0 \times 10^{-3}$
$A$	1.0	$3.3 \times 10^{-3}$	1.0	$5.4 \times 10^{-3}$

$w_0$	present e.o.s. of dark energy
$w_\infty$	asymptotic past e.o.s. of dark energy
$h$	present value of Hubble parameter
$\Omega_B h^2$	fractional baryon density $\times h^2$
$\Omega_C h^2$	fractional CDM density $\times h^2$
$A_S$	density perturbation amplitude
$n_S$	perturbation spectral index
$\tau$	reionization optical depth

All the cosmological parameters, except the dark energy ones for the SUGRA case, are chosen consistently with the current observations of CMB and large scale structure [9]. The values of all parameters are listed in the first and third column of Tab. I.

Another relevant issue is represented by degeneracies; as we specified in the previous Section, the CMB spectra not involving the BB one, namely  $\mathcal{C}^{TT}$ ,  $\mathcal{C}^{TE}$  and  $\mathcal{C}^{EE}$ , are affected by a projection degeneracy concerning the distance to the last scattering surface. Indeed, there is a curve in the plane  $(w_0, w_\infty)$  for which  $d_{LS}$  in (8) is the same, resulting in a strong degeneracy of these two parameters. Therefore, if those three power spectra were the only statistical data taken into account, the reliability of the Fisher matrix method itself would be jeopardized, since one of the conditions for its applicability is for the parameters to be as uncorrelated as possible. In this respect, the addition of the BB power spectrum, which introduces an amplitude effect and thus removes this degeneracy, has to be seen not only as an improvement

in the statistical quality of the data, but first of all as a conceptual achievement ensuring the goodness of the analysis method.

The results of the analysis are shown in the second and fourth column of table I, reporting the  $1 - \sigma$  marginalized errors for each parameter, according to the present Fisher matrix approach. For the  $\Lambda$ CDM model there is an important indication of an achievable precision between 10% and 15% for both the dark energy parameters  $w_0$  and  $w_\infty$ , while the accuracy on the others is in agreement with previous similar analysis. This was indeed expected because the BB modes statistics have large error bars and trace the physics at late redshifts so that their influence on other parameters is smaller. Results are even better for the SUGRA model, for which the precision on  $w_0$  and  $w_\infty$  is respectively of roughly 5% and between 2% and 3%; this can be attributed to the violent redshift behavior of the equation of state of this model, making it utterly sensitive to the physics probed by lensing. In the next Section we further comment these results.

## V. CONCLUSIONS

In this paper we have exploited the potentiality of the CMB physics, with particular regard to the BB modes of the polarization, which are sourced by gravitational lensing of cosmic structures, in order to constrain the dark energy dynamics at the epoch of equivalence with the non-relativistic matter component. We focus on the amplitude of the BB angular power spectrum; BB mapping techniques isolating the lensing power [18] might also be considered for extracting information about the cosmic expansion rate redshift behavior. We have shown how the BB modes, being directly linked to the cosmic dynamics and linear perturbation growth rate when dark energy enters the cosmic picture, present an enhanced sensitivity to the value of the dark energy equation of state at the corresponding epoch. Such feature breaks the so called projection degeneracy, affecting the TT, TE and EE spectra, preventing the possibility of constraining the redshift dependence of the dark energy equation of state from CMB. Indeed, the amplitude of the BB angular power spectrum is lowered by a factor as large as 30% if the equation of

state of the dark energy at high redshifts is raised to the value of typical Quintessence models, currently allowed by observations, while the TT, TE, EE spectra undergo a tiny shift in the acoustic peaks location. The reasons are that, on one hand, the lensing probes only intermediate redshifts between source and observers, and on the other, that the lensing dominates the BB power.

We have then quantified the scientific impact of our result in terms of the achievable precision on the cosmological parameters, evaluated through a Fisher matrix analysis, modeling our assumptions on the specifics of the forthcoming probes of CMB polarization, for Cosmological Constant and highly dynamical dark energy scenarios. The results are strongly encouraging, predicting an accuracy between 10 and 15% on both the present value of the dark energy equation of state and its first derivatives with respect to the scale factor, with an indication of better results for the case of a higher dark energy dynamics. This result is comparable with the one quoted in the recent paper [13], where the authors take into account SNIa data and CMB physics but do not include BB modes into the analysis and with the forecasts in [12], where the authors consider SNIa data and weak lensing of background galaxies. In particular, the prediction of a smaller uncertainty for high dark energy dynamics is reproduced also for the observable considered here. The latter might be a complementary and independent dark energy probe with respect to the ones mentioned above. In conclusion, the weak lensing of the CMB is therefore confirmed as a potential probe of the dark energy dynamics when acceleration starts, independently of the present expansion rate. This adds even more interest to the impact of high precision weak lensing measurements in cosmology [11]. Moreover, our results indicate that the measure of the dark energy dynamics suggested here could be achieved by the forthcoming CMB probes aiming at the detection of the polarization BB modes.

## VI. ACKNOWLEDGMENTS

We thank Julien Lesgourgues, Samuel Leach and Matias Zaldarriaga for useful conversations and suggestions.

---

[1] T. Padmanabhan, *Phys. Rep.* **380**, 235 (2003).

[2] P.J.E. Peebles, B. Ratra *Rev. Mod. Phys.* **75**,

- 559 (2003).
- [3] S. Perlmutter et al., *Astrophys. J.* 517, 565 (1999).
- [4] A. G. Riess et al., *Astrophys. J.* 116, 1009 (1998).
- [5] D. N. Spergel et al., *Astrophys. J. Supp.* **148**, 97 (2003).
- [6] C. Wetterich, *Nucl. Phys. B* **302**, 668 (1988).
- [7] B. Ratra and P.J.E. Peebles, *Phys. Rev. D* **37**, 3406 (1988).
- [8] P. Brax and J. Martin, *Phys. Rev. D* **61**, 103502 (2000).
- [9] M. Tegmark et al., *Phys. Rev. D* **69**, 103501 (2004).
- [10] M. Bartelmann and P. Schneider, *Phys. Rep.* **340**, 291 (2001).
- [11] A. Refregier, *Ann. Rev. Astron. Astrophys.* **41**, 645 (2003).
- [12] J. Albert et al. for the SNAP collaboration, preprint available at [babbage.sissa.it/abs/astro-ph/0507460](http://babbage.sissa.it/abs/astro-ph/0507460) (2005).
- [13] Ch. Yeche et al., submitted to *Astron. & Astrophys.*, preprint available at [babbage.sissa.it/abs/astro-ph/0507170](http://babbage.sissa.it/abs/astro-ph/0507170) (2005).
- [14] Y.-S. Song, L. Knox, *Phys. Rev. D* **70**, 063510 (2004).
- [15] B. Jain, A. Taylor, *Phys. Rev. Lett.* **91**, 141302 (2003).
- [16] W. Hu, *Phys. Rev. D* **66**, 043007 (2000).
- [17] M. Zaldarriaga and U. Seljak, *Phys. Rev. D* **58**, 023003 (1998).
- [18] C. Hirata and U. Seljak, *Phys. Rev. D* **68**, 083002 (2003).
- [19] Lewis A., *Phys. Rev. D* **71**, 083008 (2005).
- [20] K.M. Smith, W. Hu and M. Kaplinghat, *Phys. Rev. D* **70**, 043002 (2004).
- [21] M. Kaplinghat, L. Knox and Y. Song, *Phys. Rev. Lett.* **91**, 241301 (2003).
- [22] F. Giovi, C. Baccigalupi, F. Perrotta, *Phys. Rev. D* **71**, 103009 (2005).
- [23] V. Acquaviva, C. Baccigalupi and F. Perrotta, *Phys. Rev. D* **70**, 023515 (2004).
- [24] J. Hwang, *Astrophys. J.* **375**, 443 (1991).
- [25] G. Esposito-Farese and D. Polarski, *Phys. Rev. D* **63**, 063504 (2001).
- [26] F. Perrotta, C. Baccigalupi and S. Matarrese, *Phys. Rev. D* **61**, 023507 (2000).
- [27] C. Schimd, J.-P. Uzan, A. Riazuelo, *Phys. Rev. D* **71**, 083512
- [28] U. Seljak and M. Zaldarriaga, *Astrophys. J.* **469**, 437 (1996).
- [29] C. Baccigalupi, S. Matarrese and F. Perrotta, *Phys. Rev. D* **62**, 123510 (2000).
- [30] C. Baccigalupi and F. Perrotta, *Phys. Rev. D* **59**, 123508 (1999).
- [31] E.V. Linder, *Phys. Rev. Lett.* **90**, 091301 (2003).
- [32] J.A. Peacock and S.J. Dodds, *MNRAS* **267**, 1020 (1994).
- [33] C.P. Ma, R.R. Caldwell, P. Bode and L. Wang, *Astrophys. J. Lett.* **521**, L1 (1999).
- [34] H. Kodama and M. Sasaki, *Prog. Theor. Phys. Suppl.* 78, 1 (1984).
- [35] A.R. Liddle, R.J. Scherrer, *Phys. Rev. D* **59**, 023509 (1999).
- [36] P.J. Steinhardt, L. Wang, I. Zlatev, *Phys. Rev. D* **59**, 123504 (1999).
- [37] M. Bartelmann, F. Perrotta, C. Baccigalupi, *Astron. & Astrophys.* **396**, 21 (2002).
- [38] B. Gold, *Phys. Rev. D* **71**, 063522 (2005)
- [39] M. Zaldarriaga and U. Seljak, *Phys. Rev. D* **55**, 1830 (1997).
- [40] P. Oxley et al. 2004, Earth Observing System IX. Edited by William L. Barnes and James J. Butler, Proceedings of the SPIE, 5543, 320